(16) Oref, I.; Tardy, D. C. *Chem. Rev.* **1990**, *30*, 1407.
(17) Yaws, C. L. *Physical Properties*; McGraw-Hill: New York, 1978.
(18) Bayley, R. T.; Cruickshank, F. R.; Pugh, D.; Guthrie, R.; Johnstone, W.; Mayer, J.; Middleton, K. *J. Chem. Phys.* **1982**, *77*, 3453.
(19) McLafferty, F. W. *Anal. Chem.* **1962**, *34*, 2.
(20) Morrison, R. T.; Boyd, R. N. *Organic Chemistry*; Allyn and Bacon: Boston, 1973.
(21) Seakins, P. W.; Pilling, M. J. *J. Phys. Chem.* **1991**, *95*, 9874.
(22) Bethune, D. S.; Lankard, J. R.; Sorokin, P. P.; Shell-Sorokin, A. J.; Plecenik, R. M.; Avouris, Ph. *J. Chem. Phys.* **1981**, *75*, 2231.

Scanning Electrochemical Microscopy. 16. Study of Second-Order Homogeneous Chemical Reactions via the Feedback and Generation/Collection Modes

Feimeng Zhou, Patrick R. Unwin,† and Allen J. Bard*

Department of Chemistry and Biochemistry, The University of Texas at Austin, Austin, Texas 78712
(Received: January 2, 1992; In Final Form: March 6, 1992)

The application of the scanning electrochemical microscope feedback and generation/collection (G/C) modes in the measurement of second-order homogeneous reactions of electrogenerated species (i.e., the E_rC_{2i} mechanism) is considered, with particular emphasis on dimerization. Two G/C modes are assessed: (i) tip generation/substrate collection (TG/SC) and (ii) substrate generation/tip collection (SG/TC). The TG/SC mode is shown to be preferable for kinetic studies in terms of the higher collection efficiencies attainable under steady-state conditions. A numerical treatment of the feedback and TG/SC problem, which relates the tip (feedback) and substrate (collection) currents to the tip–substrate separation, the electrode radii, and dimerization rate constant, is developed, and an extensive set of calculated steady-state feedback and collection characteristics is presented that allow construction of appropriate working curves. The theoretical results suggest that fast dimerization rate constants, up to 4×10^8 M^{-1} s^{-1} (defined in terms of the rate of loss of the monomer), should be accessible to measurement in the steady-state TG/SC mode. The application of the proposed methodology is demonstrated through studies of the reductive coupling of both dimethyl fumarate (DF) and fumaronitrile (FN) in *N,N*-dimethylformamide. Good agreement between theory and experiment is displayed over a wide range of concentrations, yielding mean values for the dimerization rate constants of 170 M^{-1} s^{-1} (DF) and 2.0×10^5 M^{-1} s^{-1} (FN).

Introduction

Recent papers have demonstrated that the feedback mode of the scanning electrochemical microscope[1,2] (SECM) is useful in studying the kinetics and mechanisms of reactions associated with electrode processes,[3-5] in addition to the surface imaging and fabrication capabilities of the device.[2] Experimental studies have been conducted, and theoretical treatments developed, for both irreversible and quasi-reversible heterogeneous electron-transfer processes[3,4] and first-order homogeneous chemical reactions following the electron-transfer reaction.[5] The SECM configuration has been shown to be particularly attractive for studying fast kinetics because of the high rates of mass transfer attainable at close tip–substrate separations (down to fractions of a micrometer).

The aim of this paper is to extend the application of the SECM, as a device for electrochemical kinetics investigations, by addressing theoretically and experimentally the application of both the feedback and generation/collection (G/C) modes in the study of second-order homogeneous chemical reactions following reversible electron transfer, i.e., the E_rC_{2i} mechanism.[6] Particular attention is given to the following scheme where the chemical step is a dimerization process with a rate constant, k_c, written here for a cathodic process.

$$\text{electrode:} \quad \text{Ox} + ne^- \rightleftarrows \text{Red} \ (E_r) \tag{1}$$

$$\text{solution:} \quad 2\text{Red} \rightarrow \text{products} \ (C_{2i}) \tag{2}$$

This general scheme is of significance in a number of electrode reaction mechanisms.[6]

The principle behind the use of feedback SECM for measuring coupled homogeneous chemical reactions has been discussed previously[5] and is illustrated in Figure 1. For the E_rC_{2i} process, eqs 1 and 2, the tip ultramicroelectrode (UME) is held at a potential at which Red is generated at a diffusion-controlled rate. This establishes a competition between (i) the diffusion of Red to the conductive substrate, with the consequent regeneration and feedback diffusion of Ox, and (ii) the dimerization of Red to products (which are electroinactive at the potentials of interest), which diminishes the flux of Red at the substrate. At close tip–substrate separations, d (within about a UME diameter), the former process serves to increase the UME current, as compared to the steady-state current at the UME at long distances from the substrate (greater than about 5 UME diameters). In contrast, the overall effect of the homogeneous reaction is to consume Red and so decrease the UME feedback current. The solution kinetics are determined by measuring the UME current as a function of the tip–substrate distance (which governs the tip–substrate diffusion time, of the order of d^2/D, where D is the diffusion coefficient of Red).

In addition to the feedback mode, two SECM G/C modes are feasible, with the tip UME/substrate electrode pair operating in either the substrate generating/tip collecting (SG/TC) or tip generating/substrate collecting (TG/SC) modes (Figure 1). The latter G/C mode is similar to the feedback mode, except that now both the tip and substrate electrode currents are measured. For both G/C modes the generator electrode is held at a potential corresponding to the diffusion-controlled formation of the intermediate Red, with the potential of the collector electrode at a value where the oxidation of Red is diffusion-controlled. For the E_rC_{2i} process, eqs 1 and 2, in the TG/SC mode:

$$\text{tip:} \quad \text{Ox} + ne^- \rightarrow \text{Red} \tag{3}$$

$$\text{gap:} \quad 2\text{Red} \rightarrow \text{products} \tag{4}$$

$$\text{substrate:} \quad \text{Red} - ne^- \rightarrow \text{Ox} \tag{5}$$

In the SG/TC mode, the reaction in eq 3 occurs at the substrate and that in eq 5 at the tip.

Neither of the G/C modes have previously been employed for detailed quantitative kinetic studies of homogeneous or heterogeneous processes. However, the SG/TC mode described above

† Present address: Department of Chemistry, University of Warwick, Coventry CV4 7AL, U.K.

0022-3654/92/2096-4917$03.00/0

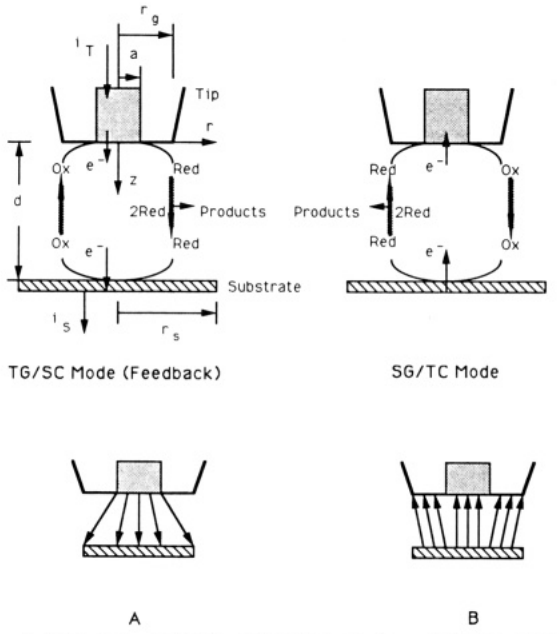

Figure 1. Principles of (A) the TG/SC feedback and (B) the SG/TC SECM modes in studying dimerization kinetics of electrogenerated species. The upper schematics show the electrode and chemical and diffusive processes within the tip–substrate domain for each case, along with the relevant coordinate system and notation. Note that for feedback measurements in the TG/SC mode, only the tip UME current is recorded. The TG/SC mode is characterized by much higher collection efficiencies than the SG/TC mode as a consequence of the relative sizes of the tip and substrate electrodes (as illustrated by the lower figures for A and B).

was used by Engstrom and co-workers[7,8] to collect short-lived intermediates at a UME and estimate the rate of associated homogeneous chemical reactions within the diffusion field of a conventional-sized generator electrode. Recently, Anson and co-workers[9] showed that, for couples uncomplicated by homogeneous chemical reactions, the TG/SC mode is characterized by extremely high collection efficiencies (a substrate current, i_S, to UME tip current, i_T, ratio of effectively unity) even at relatively large tip–substrate separations (of the order of the tip diameter).

In this paper we consider the application of both the feedback and G/C SECM modes for studying second-order homogeneous kinetics. In the case of G/C measurements, particular emphasis is given to the TG/SC mode, which is especially attractive given the potentially high collection efficiencies[9] and the ease of making steady-state measurements as compared to the SG/TC mode (as will be demonstrated below). Theoretical treatments of these cases are developed numerically by extending the alternating direction implicit (ADI) finite difference method,[10] which has proved to be suitable for modeling a variety of SECM problems.[4,5,11] Experiments involving the anion radical dimerization of dimethyl fumarate and fumaronitrile in *N,N*-dimethylformamide are employed to demonstrate the applicability of SECM feedback and G/C experiments in measuring dimerization kinetics of electrogenerated species and to test the theoretical predictions.

Theory

Formulation of the Problem. This paper is mainly concerned with feedback and TG/SC measurements under steady-state conditions. However, we have demonstrated previously that the transient (chronoamperometric) SECM behavior can provide complementary information to steady-state measurements in kinetic studies.[4,5] Thus, for completeness, we consider here the theory of feedback and TG/SC chronoamperometry, and derive the steady-state characteristics from the behavior developed at long times.

Although experimental results for the SG/TC mode are reported later in this paper, a theoretical treatment of this method is not considered here for several reasons. First, under the general conditions of SG/TC experiments, which involve a conventional (of the order of millimeters) substrate electrode (as used here and also in refs 7 and 8), steady-state measurements are precluded, because a steady-state substrate diffusion current cannot be attained for these size electrodes. Moreover, the theoretical description of such a time-dependent problem is probably more complicated than for the TG/SC mode and may require the treatment of mass transfer to the UME within a changing diffusion field at the substrate electrode, itself perturbed by the presence of the UME particularly under long time conditions. Given these considerations, and the lower collection efficiencies of this electrode arrangement, the SG/TC mode does not appear to offer any advantages over the TG/SC mode for quantitative kinetic measurements, although it may be useful in imaging substrates.

For the E_rC_{2i} mechanism, eqs 1 and 2, the relevant time-dependent diffusion equations for species Red and Ox appropriate to the SECM geometry, in cylindrical coordinates, are of the form

$$\frac{\partial c_{Ox}}{\partial t} = D_{Ox}\left[\frac{\partial^2 c_{Ox}}{\partial r^2} + \frac{1}{r}\frac{\partial c_{Ox}}{\partial r} + \frac{\partial^2 c_{Ox}}{\partial z^2}\right] \quad (6)$$

$$\frac{\partial c_{Red}}{\partial t} = D_{Red}\left[\frac{\partial^2 c_{Red}}{\partial r^2} + \frac{1}{r}\frac{\partial c_{Red}}{\partial r} + \frac{\partial^2 c_{Red}}{\partial z^2}\right] - k_c c_{Red}^2 \quad (7)$$

where r and z are, respectively, the coordinates in the directions radial and normal to the electrode surface starting at its center, D_i and c_i are the diffusion coefficient and concentration of the species i (i = Ox, Red), and t is time. The corresponding boundary conditions for both the feedback and TG/SC modes are

$$z = 0,\ 0 \le r \le a: \quad c_{Ox} = 0,\ D_{Ox}\partial c_{Ox}/\partial z = -D_{Red}\partial c_{Red}/\partial z \quad (8)$$

$$z = 0,\ a \le r \le r_g: \quad D_{Red}\partial c_{Red}/\partial z = D_{Ox}\partial c_{Ox}/\partial z = 0 \quad (9)$$

$$z = d,\ 0 \le r \le r_g: \quad c_{Red} = 0,\ D_{Red}\partial c_{Red}/\partial z = -D_{Ox}\partial c_{Ox}/\partial z \quad (10)$$

$$r \ge r_g,\ 0 \le z \le d: \quad c_{Ox} = c_{Ox}^*,\ c_{Red} = 0 \quad (11)$$

$$r = 0,\ 0 < z < d: \quad D_{Red}\partial c_{Red}/\partial r = D_{Ox}\partial c_{Ox}/\partial r = 0 \quad (12)$$

The assumptions underlying eqs 8–12 were delineated previously.[5,12] It should additionally be noted that in writing eq 10, the radius of the substrate electrode (r_s) has been assumed to be at least as large as the radius of the insulating sheath on the UME (r_g). For the values of $R_g = r_g/a$ appropriate to this work (R_g = 10), and practical tip–substrate separations, this is sufficiently large to ensure that all of species Red reaching the substrate is collected (and subsequently fed back to the UME). The minimum substrate electrode size necessary for these collection conditions to apply has important practical implications for TG/SC measurements and is discussed further below. The same results will apply for larger substrate electrodes ($r_s \gg r_g$) in the TG/SC mode. The initial condition, completing the definition of the problem, is

$$t = 0,\ 0 \le r,\ 0 \le z \le d: \quad c_{Ox} = c_{Ox}^*;\ c_{Red} = 0 \quad (13)$$

To obtain general solutions, the problem can be cast into dimensionless form through the introduction of the following variables:

$$R = r/a \quad (14)$$

$$Z = z/a \quad (15)$$

$$C_i = c_i/c_{Ox}^* \quad (16)$$

$$\tau = tD/a^2 \quad (17)$$

$$K = k_c a^2 c_{Ox}^*/D \quad (18)$$

As before,[4,5,12] the last two equations imply that only the case where $D = D_{Red} = D_{Ox}$ will be considered here.

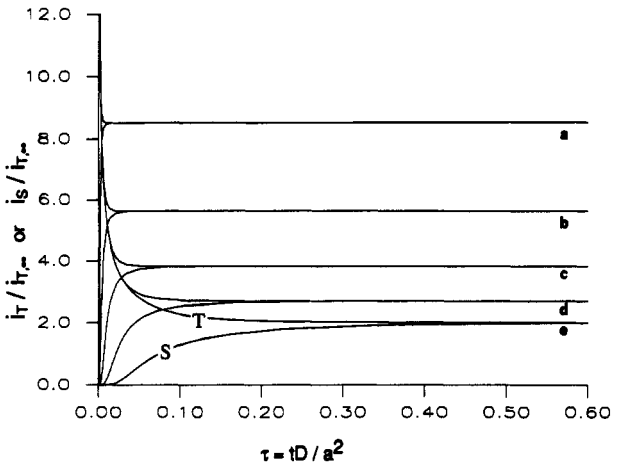

Figure 2. SECM tip and substrate (magnitudes) chronoamperometric characteristics for diffusion-controlled conditions in the absence of following chemical kinetics. The data are for log (d/a) = (a) −1, (b) −0.8, (c) −0.6, (d) −0.4, and (e) −0.2. The tip and substrate currents are denoted by T and S on curves e.

The aim of the calculations is to determine both the UME and substrate current responses as a function of time, t. Note, however, that only the UME current is required to define the feedback characteristics. The magnitude of both currents is evaluated from

$$i_T = nFD\int_0^a 2\pi r(\partial c_{Ox}/\partial z)_{z=0}\,dr \qquad (19a)$$

$$i_S = nFD\int_0^{r_s} 2\pi r(\partial c_{Red}/\partial z)_{z=d}\,dr \qquad (19b)$$

where F is the Faraday. Convenient dimensionless forms for eq 19 are

$$(i_T/i_{T,\infty}) = (\pi/2)\int_0^1 (\partial C_{Ox}/\partial Z)_{Z=0} R\,dR \qquad (20a)$$

$$(i_S/i_{T,\infty}) = (\pi/2)\int_0^{R_s} (\partial C_{Red}/\partial Z)_{Z=d/a} R\,dR \qquad (20b)$$

The denominator on the left-hand side of eq 20 denotes the steady-state current at a simple ultramicrodisk electrode:[13]

$$i_{T,\infty} = 4nFDc_{Ox}{}^{*}a \qquad (21)$$

Method of Solution. The equations above were solved numerically by the alternating direction implicit (ADI) finite difference method,[10] which is an efficient technique for tackling a variety of SECM problems.[4,5,11] A general description of the method is given elsewhere;[5] brief additional details relevant to the present problem are given in the supplementary material.

Theoretical Results and Discussion

Behavior in the Absence of Homogeneous Kinetics. It is useful to briefly consider the SECM feedback and TG/SC characteristics (under diffusion-controlled conditions) in the absence of following homogeneous kinetics. The chronoamperometric feedback behavior for this situation has been discussed in detail previously.[5,14] However, the TG/SC chronoamperometric mode has not been previously treated. Typical numerical results showing the tip and substrate response for this case, at various tip–substrate separations, are shown in Figure 2. The characteristics are as expected given the form of the feedback behavior,[5,14] the smaller d, the shorter the time at which the substrate electrode current begins to flow, following the potential step at the UME tip, and the larger the magnitude of the steady-state tip (feedback) and substrate electrode currents.

For all of the tip–substrate separations (d/a) considered in Figure 2, steady-state collection efficiencies $(i_S/i_T)_{SS}$ of essentially 100% are attained. This behavior, which is characteristic of the SECM geometry, extends to large tip–substrate separations (Table I), i.e., $(i_S/i_T)_{SS} > 0.99$ when $d/a < 2$. These very high collection efficiencies result when the (normalized) tip–substrate separation (d/a) is much less than R_g. Under these conditions, diffusion of the tip-generated intermediate to the substrate (for collection), rather than escape from the tip–substrate domain, is favored. Only at comparatively longer distances does a fraction of the intermediate escape from the gap. Clearly the larger the substrate (collecting) electrode and the value of R_g, the greater the tip–substrate separation necessary to promote the loss of the intermediate from the tip–substrate domain by diffusion.

TABLE I: SECM Steady-State TG/SC Efficiencies for Diffusion-Controlled Feedback with a Stable Mediator

log (d/a)	collection efficiency, $N = i_S/i_T$	log (d/a)	collection efficiency, $N = i_S/i_T$
−1.0	1.00	0.3	0.992
−0.8	1.00	0.4	0.978
−0.6	1.00	0.5	0.973
−0.4	1.00	0.6	0.866
−0.2	1.00	0.7	0.794
0.0	0.998		

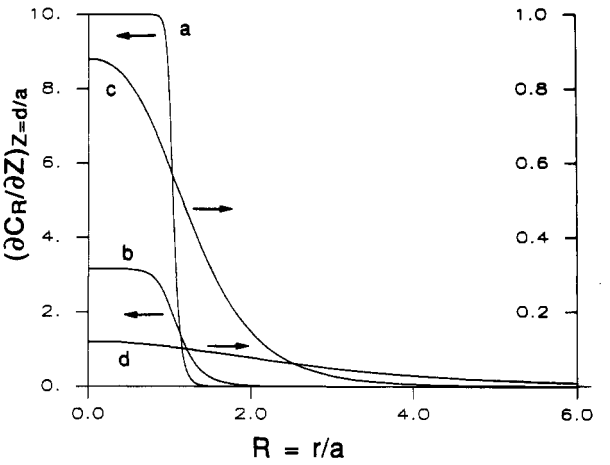

Figure 3. Normalized flux of R at the substrate electrode for diffusion-controlled kinetically-uncomplicated conditions. The data are for log (d/a) = (a) −1.0, (b) −0.5, (c) 0.0, and (d) 0.5.

It also follows that for relatively close tip–substrate separations (i.e., those leading to collection efficiencies of essentially 100%) the portion of the substrate electrode which collects the intermediate species (under steady-state conditions) depends upon the tip–substrate separation. This point is illustrated by Figure 3 which (considering the tip electrode reaction, eq 1) shows the flux of Red at the substrate electrode surface. When the separation is larger, the electrode area active in the collection process also is larger. Empirically, the distance dependence of the minimum dimensionless substrate size, $h^{\infty} = r_s/a$, required for a collection efficiency of effectively 100% is as previously deduced for the corresponding feedback problem:[4]

$$h^{\infty} = 1 + 1.5(d/a) \qquad (22)$$

Equation 22 has important experimental implications since the noise, in the form of residual current, associated with the steady-state current signal is proportional to the surface area of the electrode. This equation thus serves as a guide to the minimum electrode size which can be employed experimentally, if the highest signal-to-noise ratio is desired.

Effect of Following Dimerization Kinetics. Typical tip and substrate chronoamperometric characteristics for log $(d/a) = -0.4$ and K = 1, 10, and 100 are shown in Figure 4 along with the corresponding (kinetically uncomplicated) diffusion-controlled behavior. As expected, the tip (feedback) current behavior is qualitatively similar to that for the E_rC_i process discussed in detail previously.[5] At short times the current is close to that for positive diffusion-controlled feedback, but at times comparable to the lifetime of Red, deviation from this behavior occurs, as the following chemical reaction consumes this intermediate. The larger is the value of K, the shorter is the time at which the effect of

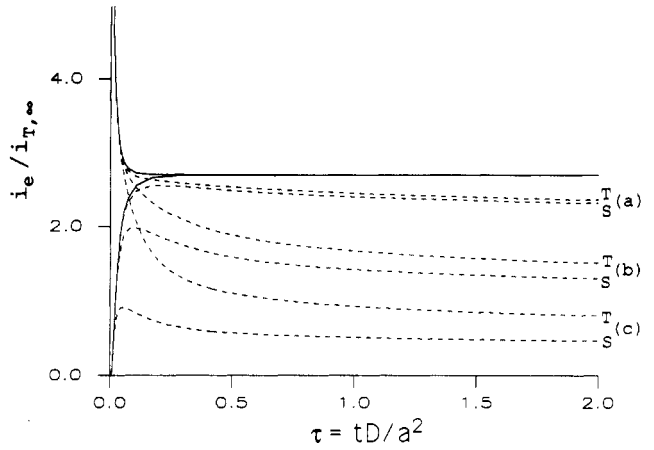

Figure 4. SECM tip and substrate chronoamperometric characteristics for the E_rC_{2i} mechanism with log $(d/a) = -0.4$. The solid line shows the behavior in the absence of following homogeneous kinetics while the labeled dashed lines are for K = (a) 1, (b) 10, and (c) 100. The labels T and S denote tip and substrate, respectively.

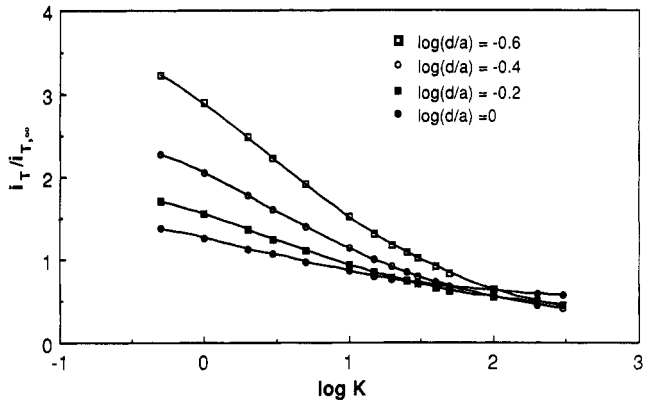

Figure 5. SECM feedback working curves for the E_rC_{2i} mechanism at various tip–substrate separations.

the chemical reaction is observed in the feedback chronoamperogram, and the smaller the value of the final steady-state tip current (typically attained at $\tau \geq 130$).

The corresponding substrate (collector) chronoamperometric characteristics, which have not been reported previously for any electrode reaction mechanism, also initially follow the behavior predicted for the kinetically uncomplicated diffusion-controlled situation (Figure 4). However, as the tip–substrate diffusion rate decreases (at longer times in the chronoamperogram), the following chemical reaction competes with the diffusion of the intermediate from the tip to the substrate, decreasing the flux of Red (and hence current) at the substrate electrode. This leads to a peak in the i_s vs t characteristic, as shown in Figure 4. In principle, the magnitude and position of this peak could be used to estimate the reaction rate. Qualitatively, the faster the following chemical reaction, the smaller is the peak current and the shorter is the time at which the peak occurs.

One of the attractive features of the SECM is its ability to study fast processes under steady-state conditions.[3-5] An extensive set of calculated tip and substrate steady-state currents, for practical tip–substrate separations and a wide range of normalized rate constants, is given in Table II; a larger table of calculated results is contained in the supplementary material. These data can be used to construct working curves for most of the experimental situations encountered in studies of the E_rC_{2i} mechanism. To illustrate the general features of the steady-state feedback characteristics, Figure 5 shows a limited set of tip current (feedback) working curves constructed from Table II for several tip–substrate separations. As expected, in each case the data tend toward the behavior for diffusion-controlled (positive) and negative (insulating substrate) feedback, in the limits of small and large K, respectively. As is now well established for SECM studies,[4,5]

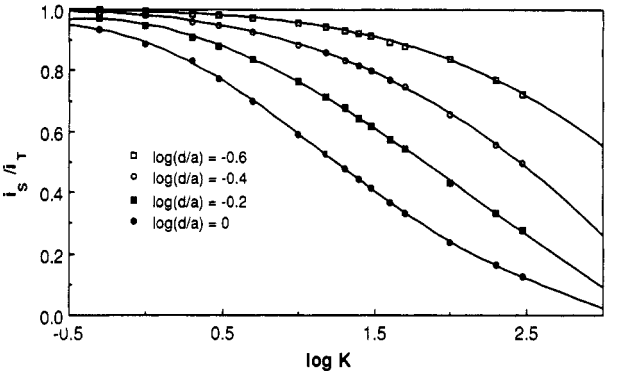

Figure 6. SECM collection efficiencies (i_S/i_T) vs K for various tip–substrate separations.

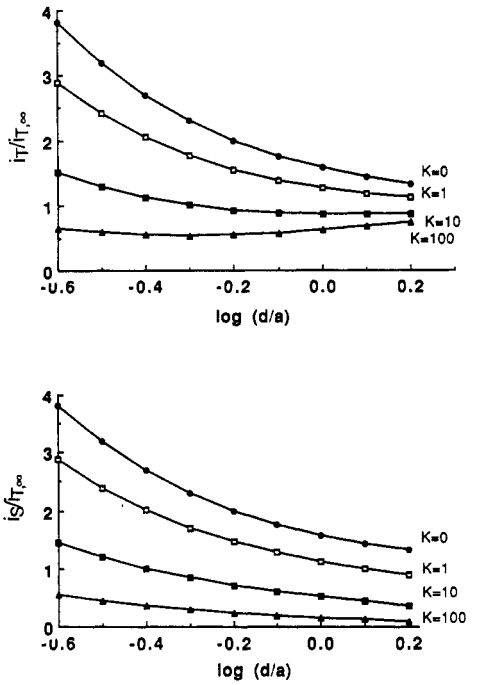

Figure 7. Simulated tip and substrate electrode current–distance curves for various values of K.

Figure 5 indicates that kinetic parameters can be determined with the highest accuracy at the closest tip–substrate separations.

The complementary steady-state TG/SC SECM characteristics are shown in Figure 6 as plots of $(i_S/i_T)_{SS}$ vs K for various normalized tip–substrate separations. As expected, the collection efficiency shows a decrease as the rate of the following chemical reaction increases, since this process consumes the tip-generated intermediate, Red, in its transit from the tip to the substrate. For a given value of K, this decrease in collection is more pronounced with a larger tip–substrate separation, i.e., with a longer diffusion time between tip and substrate.

The normalized tip and substrate current data in Table II indicates that although the following chemical reaction lowers both i_T and i_S compared to the corresponding kinetically uncomplicated diffusion-controlled cases, the collection efficiencies can approach 100% for certain values of K (compare Figures 6 and 7). This arises because the magnitude of both the tip and substrate electrode currents are decreased by the homogeneous reaction (due to the feedback process). This is to be contrasted with the situation at hydrodynamic double electrodes, such as the rotating ring–disk[15] or double channel[16] electrodes, where the generator electrode current is unaffected by following chemical reactions as there is no feedback component to the current at this electrode. Given this situation, the analysis of SECM TG/SC experimental data is probably better carried out in terms of individual normalized feedback tip and substrate collector electrode currents rather than their ratio (i.e., the formal collection efficiency).

TABLE II: Theoretical Normalized Tip and Substrate Steady-State Currents for the E_rC_{2i} Mechanism

log (d/a)	$K = 1$		$K = 5$		$K = 10$		$K = 20$		$K = 50$		$K = 100$		$K = 200$		$K = 500$		$K = 1000$		$K \to \infty$
	$i_T/i_{T,\infty}$	$i_S/i_{T,\infty}$	$i_T/i_{T,\infty}$	$i_S/i_{T,\infty}$	$i_T/i_{T,\infty}$	$i_S/i_{T,\infty}$	$i_T/i_{T,\infty}$	$i_S/i_{T,\infty}$	$i_T/i_{T,\infty}$	$i_S/i_{T,\infty}$	$i_T/i_{T,\infty}$	$i_S/i_{T,\infty}$	$i_T/i_{T,\infty}$	$i_S/i_{T,\infty}$	$i_T/i_{T,\infty}$	$i_S/i_{T,\infty}$	$i_T/i_{T,\infty}$	$i_S/i_{T,\infty}$	$i_T/i_{T,\infty}$
−0.8	4.255	4.236	2.778	2.756	2.186	2.144	1.672	1.630	1.166	1.099	0.864	0.797	0.629	0.577	0.433	0.365	0.335	0.254	0.102
−0.7	3.490	3.479	2.289	2.256	1.813	1.756	1.396	1.336	0.977	0.898	0.728	0.655	0.552	0.470	0.392	0.296	0.311	0.205	0.127
−0.6	2.889	2.873	1.909	1.860	1.517	1.448	1.180	1.098	0.834	0.734	0.639	0.536	0.498	0.382	0.369	0.239	0.303	0.164	0.159
−0.5	2.418	2.392	1.616	1.544	1.296	1.200	1.021	0.908	0.726	0.601	0.581	0.439	0.464	0.311	0.361	0.192	0.307	0.131	0.198
−0.4	2.050	2.011	1.392	1.291	1.131	1.001	0.906	0.754	0.673	0.501	0.546	0.359	0.451	0.252	0.367	0.153	0.324	0.102	0.246
−0.3	1.766	1.708	1.225	1.089	1.012	0.840	0.828	0.629	0.638	0.413	0.535	0.292	0.458	0.202	0.389	0.119	0.356	0.078	0.303
−0.2	1.549	1.468	1.105	0.925	0.931	0.708	0.779	0.526	0.628	0.339	0.545	0.236	0.484	0.160	0.430	0.091	0.403	0.058	0.371
−0.1	1.386	1.276	1.023	0.791	0.882	0.600	0.760	0.439	0.639	0.277	0.574	0.189	0.527	0.125	0.485	0.069	0.466	0.042	0.448
0.0	1.265	1.123	0.972	0.680	0.860	0.508	0.764	0.365	0.670	0.224	0.620	0.148	0.585	0.095	0.556	0.050	0.542	0.030	0.534
0.1	1.178	0.997	0.946	0.586	0.859	0.429	0.786	0.302	0.715	0.179	0.680	0.115	0.655	0.072	0.635	0.036	0.626	0.021	0.624
0.2	1.123	0.892	0.939	0.503	0.874	0.361	0.821	0.247	0.770	0.141	0.746	0.088	0.729	0.053	0.701	0.026	0.711	0.015	0.710

Since steady-state SECM kinetic studies involve measuring i_T and i_S as a function of the tip–substrate separation, it is informative to examine the overall current–distance behavior for various kinetic regimes. Figure 7 shows these characteristics for several values of K. As found previously for the E_rC_i mechanism,[5] the form of the tip (feedback) current characteristics at low K is similar to that for kinetically-uncomplicated diffusion control. For larger values of K, a minimum is observed in the i_T vs d behavior, for the reasons discussed previously.[5] In contrast, the corresponding i_S vs d characteristics show no minimum; for a given value of K the magnitude of collector current decreases monotonically as the tip–substrate distance (and hence the diffusion time) increases.

Range of Measurable Rate Constants. As discussed previously,[5] the SECM can, in principle, be used to measure rate constants over a wide range, by tuning the tip electrode radius, a (see eq 18). Given the large number of conventional electrochemical techniques available for studying dimerization processes with intermediate rates,[6] greatest interest is probably in estimating the fastest rates which can be measured with the proposed SECM methodology. In this situation, the TG/SC mode is likely to be more suitable than the feedback mode, since the former relies on the measurement of absolute currents at the tip and substrate, while in the latter, kinetic information is deduced from a small enhancement in the tip (feedback) current (see Table II).

It is apparent from Table II that relatively large normalized substrate currents result at moderate tip–substrate separations, even for $K = 1000$. For a tip UME with $a = 5$ μm, and $c^* = 10^{-4}$ M, $D = 10^{-5}$ cm^2 s^{-1}; this implies that a rate constant of 4×10^8 M^{-1} s^{-1} could be determined. This would require the measurement of substrate currents in the range of 49 pA [log (d/a) = −0.8] to 11 pA [log (d/a) = −0.2]. These values are well within the range of those accessible with present instrumentation for low current measurements. Larger rate constants could be determined, if smaller c^* levels, yielding smaller i_S values, could be used, or at smaller values of d/a. This upper estimate is over 1 order of magnitude greater than that accessible from RRDE collection efficiency measurements[15] and compares very favorably with those predicted from advanced transient techniques such as fast scan cyclic voltammetry.[17–20]

Experimental Section

Reagents. N,N-Dimethylformamide (DMF) (B&J Brand, Baxter Diagnostics Inc., McGaw Park, IL) was stored in a dry box under a He atmosphere. It was treated with neutral alumina atk-I (ICN Biochemicals Inc., Costa Mesa, CA) prior to use. N,N,N',N'-Tetramethyl-1,4-phenylenediamine (TMPD), dimethyl fumarate (DF), and fumaronitrile (FN) (all from Aldrich Chemical Co., Inc., Milwaukee, WI) were used without further purification. The supporting electrolyte, tetra-n-butylammonium tetrafluoroborate ($TBABF_4$), was recrystallized three times from acetone/ether and dried in a vacuum oven for 48 h.

Electrodes. Ultramicroelectrode tips were fabricated from either 25-μm- or 10-μm-diameter platinum wires (Goodfellow Metals, Cambridge, UK), as described previously.[1] For each electrode, the end of the glass sheath around the disk tip was further ground to yield a cone, and the tip was successively polished by finer diamond pastes to 0.25 μm on felt (Buehler Ltd., Lake Bluff, IL). The electrode/glass radius ratio, RG = r_g/a (measured optically), was close to 10. Substrates were of two different sizes. For feedback and generation/collection measurements involving DF, a 500-μm-diameter Pt electrode embedded in a glass sheath was placed flush with the base of the Teflon electrochemical cell, whereas for experiments with FN, the substrate electrode was a 100-μm-diameter Pt disk sealed in a glass tube. The substrate electrodes were polished in the same manner as the tips prior to every experimental run. A Pt wire was used as the counter electrode and a Ag wire served as a quasi-reference electrode (AgQRE).

Apparatus. The SECM instrument and electrochemical cell were described previously.[21] For the present studies, this apparatus was placed in a home-built glovebox, which was flushed with N_2 that had been passed through a column of Drierite (W. A.

Hammond Drierite Company, Xenia, OH) for 3 h prior to the experiments.

Procedure. All solutions were made up in a commercial glovebox and sealed in vials with Parafilm for transfer to the SECM glovebox. These DMF solutions contained the species of interest (either DF or FN in various concentrations), the supporting electrolyte, $TBABF_4$, and TMPD as an additional SECM mediator. TMPD was used to determine the tip–substrate separation. TMPD and $TMPD^{\bullet+}$ are both kinetically stable in these solutions, and its electron transfer processes are rapid so that comparison of the diffusion-controlled feedback characteristics to theory[12] provides an accurate independent measurement of d.

Both feedback and TG/SC experiments involved initially recording the steady-state tip current for TMPD used as the SECM mediator at a large tip–substrate separation ($d > 20a$), i.e., when $i_T = i_{T,\infty}$. The tip was then moved toward the substrate electrode, using the z-axis inchworm motor of the SECM, with the potentials of both electrodes held at values sufficient for diffusion-controlled feedback of TMPD. Once the desired separation had been attained, as judged by the feedback current of the TMPD mediator,[12] the tip potential was changed to a value where the reaction of interest (reduction of DF or FN) was diffusion-controlled (and the substrate electrode was held at a potential sufficient to oxidize tip-generated product at a diffusion-controlled rate). TMPD was inactive at these potentials at both tip and substrate. Either the tip feedback current or tip and substrate currents (TG/SC) were recorded. The tip and substrate potentials were then readjusted to values for the SECM mediator (TMPD), and the above procedure was repeated to attain a new tip–substrate separation. For very close tip–substrate separations (when $i_T > 4i_{T,\infty}$), a piezo pusher[21] rather than the inchworm motor was utilized, which allowed a finer approach of the tip to the substrate.

Results and Discussion

The proposed SECM techniques were applied to two reductive hydrodimerizations involving activated olefins.[22-29] These reactions have been studied extensively and show a wide range of radical anion dimerization rates that depend on the substituent activating the olefinic double bond. For example, for dimethyl fumarate (DF), which has been studied by a variety of electrochemical methods in DMF,[27,28] the following dimerization reaction is relatively slow, reported to range from 220 to 320 M^{-1} s^{-1}, based on the cyclic voltammetry (CV), simultaneous electrochemical-electron spin resonance (SEESR), double potential step chronocoulometry, and rotating ring–disk electrode (RRDE) steady-state generation/collection experiments. Fumaronitrile (FN), which shows much faster radical anion coupling rates, is a better test of the SECM technique, since the dimerization of $FN^{\bullet-}$ is more difficult to study with conventional electrochemical methods; estimates of 6×10^5 to 1.4×10^6 M^{-1} s^{-1} have been made based on RRDE and SEESR studies.[27,28]

Dimerization of the DF Radical Anion. For slow following chemical reactions such as the dimerization of DF radical anion, a relatively large UME is most appropriate so that the value of K is in a range where the SECM response is sensitive to the kinetics (see eq 18), thus a 25-μm-diameter Pt tip electrode and a 500-μm Pt substrate electrode were employed. Experiments were carried out with solutions of 5.15 and 11.5 mM DF in DMF containing 0.1 M $TBABF_4$ and 4.14 mM TMPD as the calibration mediator. Tip UME voltammetry at large tip–substrate separations shows reduction of DF at about −1.1 V vs AgQRE. The steady-state current yielded a value of $D = 1.04 \times 10^5$ cm^2 s^{-1} (via eq 21), which is close to that of 9.50×10^{-6} cm^2 s^{-1} deduced from RRDE voltammetry under similar conditions.[27] The one-electron oxidation of TMPD occurred at 0.3 V vs AgQRE, and the resulting tip current yielded $D = 1.2 \times 10^5$ cm^2 s^{-1}.

Both TG/SC and SG/TC modes were employed to study DF radical anion dimerization. Figures 8a and 8b show typical tip and substrate current responses for these two modes at a tip–substrate separation of 12 μm. In each case, a scan rate, v, of 100 mV/s was applied to the generator electrode (starting potential 0.0 V, with an initial sweep through the TMPD wave and then the DF wave) while the collector electrode was held at 0.0 V vs AgQRE. The latter potential was suitable for collecting both $TMPD^{\bullet+}$ (via reduction) and $DF^{\bullet-}$ (via oxidation) at a diffusion-controlled rate.

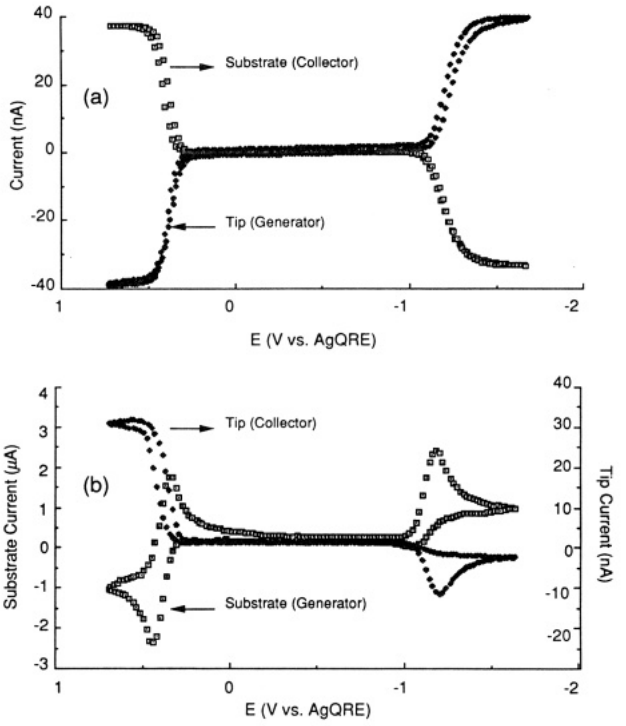

Figure 8. SECM cyclic voltammograms of TMPD and DF at a tip–substrate separation of 12 μm in (a) the TG/SC mode, where the tip is scanned to the first oxidation of TMPD and then to the reduction of DF at a scan rate of 100 mV/s with the substrate potential, E_S, held at 0.0 V vs AgQRE; and (b) the SG/TC mode where substrate is scanned at 100 mV/s with tip potential, E_T, held at 0.0 V vs AgQRE. Experimental parameters are: [DF] = 5.15 mM, [TMPD] = 4.14 mM. Curves with ◆ and □ are the tip and substrate voltammograms, respectively.

Figure 8 provides an excellent illustration of the difference between the two SECM G/C modes. In the TG/SC mode (Figure 8a) essentially steady-state tip and substrate current responses are obtained even at a tip scan rate of 100 mV/s. Moreover, as predicted by theory, almost 100% of $TMPD^{\bullet+}$ generated at the tip is collected at the substrate, and a very high collection efficiency is also found for the $DF/DF^{\bullet-}$ couple, suggesting that the follow-up chemical kinetics are relatively slow.

When the large substrate electrode serves as the generator in the SG/TC mode (Figure 8b), the response at the two electrodes is radically different. For the $TMPD/TMPD^{\bullet+}$ couple a conventional cyclic voltammogram for a nernstian process is observed as judged by values of the anodic/cathodic peak current ratio of 1.05 and peak potential separation of 67 mV (uncorrected for uncompensated resistance). The anodic substrate current is only about 10% lower than the value measured in the absence of the tip, which suggests that the UME probe does not significantly perturb the substrate electrode diffusion field on the time scale of these measurements. In contrast to the substrate, the corresponding tip (collector) current behavior response to the forward and reverse substrate potential sweeps with TMPD approaches a steady-state response and the value of the plateau current is close to the feedback current measured in the TG/SC mode (see Figure 8a). These results indicate that under the conditions of these experiments, the major mode of mass transfer is diffusion of material within the tip–substrate domain. Extensive electrolysis and consequent diffusion of material in and out of the gap is not important on the time scale of these SECM SG/TC cyclic voltammetric measurements.

For the $DF/DF^{\bullet-}$ couple, the substrate electrode cyclic voltammetric current response at this v is that expected for a couple that involves a follow-up chemical reaction, i.e., the peak current on the reverse scan is considerably diminished. The depletion of

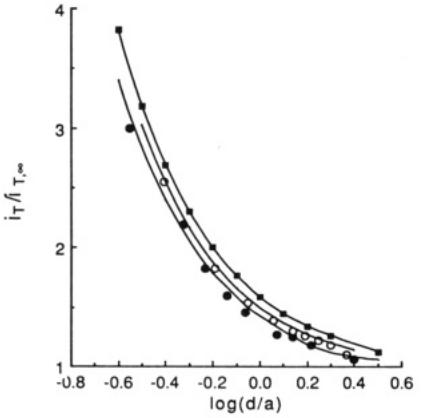

Figure 9. Normalized tip (feedback) current–distance behavior for [DF] = 5.15 mM (○) and 11.5 mM (●) along with the best theoretical fits (solid lines) for $K = 0.14$ and $K = 0.27$. The simple diffusion-controlled feedback behavior, deduced from experiments with TMPD oxidation, is also shown (■).

$DF^{\bullet-}$ in the gap region by the dimerization process also causes a decrease in the tip collector current. Additionally, since diffusion into the gap is negligible under the experimental conditions (as discussed above), the time dependence of $DF^{\bullet-}$ concentration in the tip–substrate domain prevents the establishment of a steady-state collector current, as in a dual electrode thin layer cell.[31] The large differences in the collector current responses for the two SECM G/C modes clearly illustrate the advantages of the TG/SC over the SG/TC mode in the study of following chemical reactions, in terms of both the ability to make steady-state measurements and the resulting (potentially) high collecting efficiencies. Although the employment of faster scan rates in the SG/TC mode could increase the collection current for the $DF/DF^{\bullet-}$ system, this technique probably would not offer any advantages over other transient methods, such as fast scan cyclic voltammetry, in the study of relatively fast following chemical reactions.

Typical feedback current–distance curves, obtained by holding the tip potential at a value for either the diffusion-controlled reduction of DF or the oxidation of TMPD, and the substrate potential at 0.0 V vs AgQRE, which is sufficient to collect tip product for both processes at a diffusion-controlled rate, are shown in Figure 9. The experimental data for both concentrations of DF are observed to lie slightly below the behavior predicted for simple diffusion-controlled feedback (deduced from the experiments of TMPD oxidation). This is diagnostic of a relatively slow following homogeneous reaction, on the time scale of SECM steady-state measurements. The curves through the experimental tip current data are the best fits to the theoretical model for the E_rC_{2i} mechanism for normalized rate constants of 0.14 (5.15 mM) and 0.27 (11.5 mM). Both experimental sets of data agree well with the theoretical predictions, and yield rate constants of 180 M^{-1} s^{-1} and 160 M^{-1} s^{-1}, respectively, for the dimerization process. These values are in good agreement with the rate constants measured by other electrochemical methods, discussed above. Complementary tip and substrate TG/SC current–distance curves, obtained with [DF] = 5.15 mM, are shown in Figure 10, along with the corresponding theoretical best fit for $K = 0.14$. The good level of agreement between the experimental and theoretical characteristics indicates that the TG/SC mode provides a good quantitative measurement of the rate constant of the second-order chemical reaction.

Dimerization of FN Radical Anion. As discussed above, the estimated rate constant for $FN^{\bullet-}$ dimerization is relatively high, and thus a 10-μm-diameter Pt tip and 100-μm Pt substrate were employed in these studies. Experiments were carried out with four different concentrations of FN (1.5, 4.1, 28.2, and 121 mM) in DMF. A supporting electrolyte concentration of 0.1 M was used for the first three solutions, but this was increased to 0.5 M for the highest concentration of FN to minimize effects arising from the migration of $FN^{\bullet-}$. TMPD (9.5 mM) was again em-

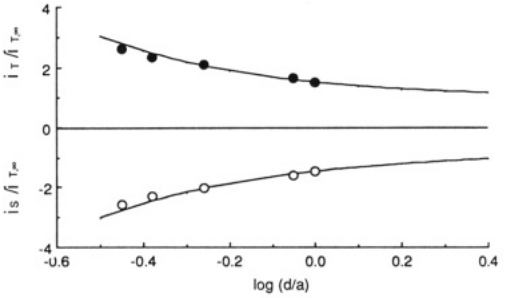

Figure 10. Normalized tip (feedback, ●) and substrate (collection, ○) currents for DF reduction (5.15 mM) as functions of tip–substrate separations in the G/C mode. The solid lines representing the behavior for $K = 0.14$ are close to those predicted for simple diffusion-controlled feedback and G/C, demonstrating that the following chemical reaction is slow on the time scale of the SECM measurements.

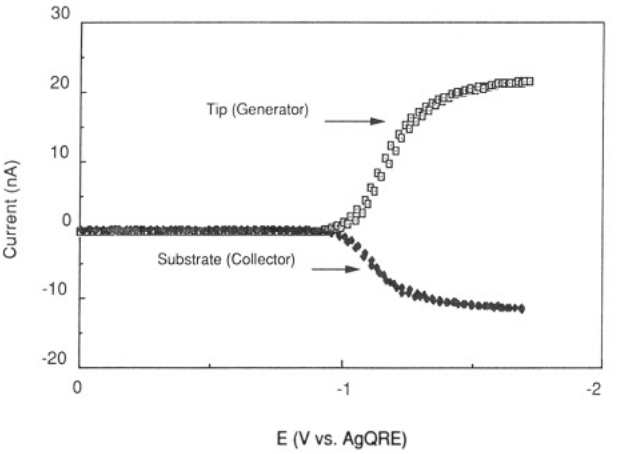

Figure 11. SECM voltammograms for FN (28.2 mM) reduction in the TG/SC mode at a tip–substrate separation of 1.8 μm, where the tip was scanned at 100 mV/s with $E_S = 0.0$ V vs AgQRE. Curves with □ and ◆ denote the tip and substrate voltammograms, respectively.

ployed as the SECM calibration mediator. UME voltammetric measurements carried out at a large tip–substrate separation indicated that the half-wave potential for the reduction of FN is about −1.1 V vs AgQRE. The steady-state diffusion limited current yielded a value of $D = 7.1 \times 10^{-6}$ cm^2 s^{-1} (via eq 22), which is in good agreement with that of 6.5×10^{-6} cm^2 s^{-1} deduced from RRDE studies.[27]

Although it has been reported that the reduction of FN in very dry DMF leads to filming of the electrode,[27] attributable to a possible polymerization process, we found that this was not a serious problem. The electrode response sometimes decreased slightly (~10%, as judged by the diffusion-limited current) over extended measurement periods. When this occurred, the electrode could be activated by scanning to potentials of about +2.5 V vs AgQRE.

Typical TG/SC tip and substrate responses for a 28.2 mM FN and a tip–substrate separation of 1.8 μm are shown in Figure 11. These were recorded by scanning the tip (generator) potential at 100 mV/s from 0.0 V through the $FN/FN^{\bullet-}$ wave while holding the substrate (collector) electrode at 0.0 V vs AgQRE to collect the intermediate, $FN^{\bullet-}$. Even though the following dimerization of $FN^{\bullet-}$ is known to be relatively fast, large steady-state (feedback) tip and (collector) substrate currents result, providing a clear illustration of the ability of this SECM mode to measure fast homogeneous processes. The feedback and collection TG/SC current–distance behavior for the four different FN concentrations are shown in Figures 12a and 12b. The best theoretical fits of those data were obtained with $K = 10$ (1.5 mM), 25 (4.1 mM), 200 (28.2 mM), and 1000 (121 mM), which correspond to dimerization rate constants of 1.9×10^5, 1.7×10^5, 2.0×10^5, and 2.4×10^5 M^{-1} s^{-1}, respectively. The consistency of this rate constant over almost 2 orders of magnitude in FN concentration provides clear evidence of the second-order nature of the following

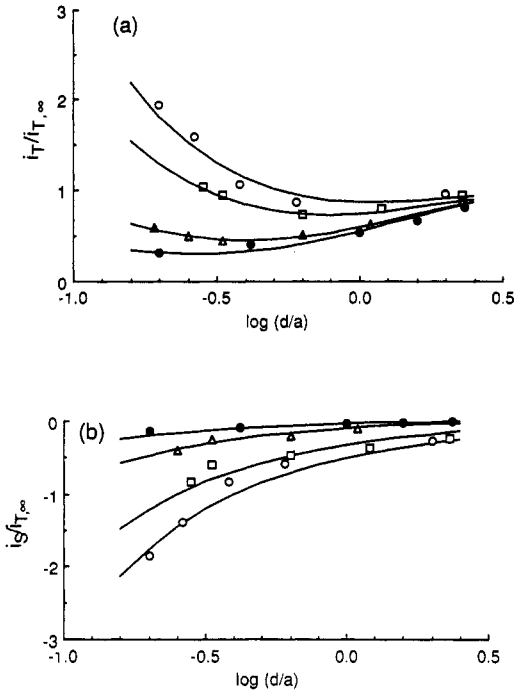

Figure 12. Normalized tip (generation, a) and substrate (collection, b) current–distance behavior for [FN] = 1.5 mM (○), 4.12 mM (□), 28.2 mM (△) and 121 mM (●); a = 5 μm, r_s = 50 μm. The solid lines through each of the data sets indicate the best theoretical fits with the values of K cited in the text.

chemical reaction of $FN^{\bullet-}$. This value is in reasonable agreement with that of $(6 \pm 3) \times 10^5$ M^{-1} s^{-1} estimated from SEESR studies, but much lower than the rate constant measured by RRDE collection efficiency experiments.[28] The higher sensitivity (i.e., significantly larger collection efficiencies) of the TG/SC SECM technique suggests that this measured value for k_c is more accurate than that deduced from RRDE measurements.

Conclusions

This study has demonstrated that the dimerization kinetics of electrogenerated species can readily be studied via the steady-state feedback and G/C modes of the SECM. The high level of agreement between theory and experiments involving the reductive coupling of both dimethyl fumarate and fumaronitrile demonstrates the validity of the SECM methodology for the proposed studies and suggests that the SECM response is theoretically well-modeled for this situation. The steady-state TG/SC mode, in particular, appears to be attractive for measuring fast chemical reactions. Rate constants of the order of 4×10^8 M^{-1} s^{-1} should be accessible to measurement, which is in excess of those attainable via collection efficiency measurements at hydrodynamic double electrodes, such as the RRDE[15] or DCE,[16] and comparable to those measurable with fast scan cyclic voltammetry without the need for complex current measurement instrumentation, background correction procedures, and contributions from adsorbed reactant or intermediates.

Acknowledgment. The support of this research by the Robert A. Welch Foundation is gratefully acknowledged. P.R.U. thanks SERC for the award of a NATO Fellowship.

Registry No. DMF, 68-12-2; TMPD, 100-22-1; DF, 624-49-7; FN, 764-42-1; $TBABF_4$, 429-42-5; $DF^{\bullet-}$, 34516-76-2; $FN^{\bullet-}$, 62600-65-1; Pt, 7440-06-4.

Supplementary Material Available: Details of the numerical solution and an extended table of the results presented in Table II (6 pages). Ordering information is given on any current masthead page.

References and Notes

(1) Bard, A. J.; Fan, F.-R. R.; Kwak, J.; Lev, O. *Anal. Chem.* **1989**, *61*, 132.
(2) (a) Bard, A. J.; Denault, G.; Lee, C.; Mandler, D.; Wipf, D. O. *Acc. Chem. Res.* **1990**, *23*, 257. (b) Bard, A. J.; Fan, F.-R. R.; Pierce, D. T.; Unwin, P. R.; Wipf, D. O.; Zhou, F. *Science* **1991**, *254*, 68.
(3) Wipf, D. O.; Bard, A. J. *J. Electrochem. Soc.* **1991**, *138*, 469.
(4) Bard, A. J.; Mirkin, M. V.; Unwin, P. R.; Wipf, D. O. *J. Phys. Chem.* **1992**, *96*, 1861.
(5) Unwin, P. R.; Bard, A. J. *J. Phys. Chem.* **1991**, *95*, 7814.
(6) Bard, A. J.; Faulkner, L. R. *Electrochemical Methods*; Wiley: New York, 1980.
(7) Engstrom, R. C.; Weaver, M.; Wunder, D. J.; Burgess, R.; Winquist, S. *Anal. Chem.* **1986**, *58*, 844.
(8) Engstrom, R. C.; Meaney, T.; Tople, R.; Wightman, R. M. *Anal. Chem.* **1987**, *59*, 2005.
(9) Lee, C.; Kwak, J.; Anson, F. C. *Anal. Chem.* **1991**, *63*, 1501.
(10) Peaceman, D. W.; Rachford, H. H. *J. Soc. Ind. Appl. Math.* **1955**, *3*, 28.
(11) Unwin, P. R.; Bard, A. J. *J. Phys. Chem.* **1992**, *96*, 5035.
(12) Kwak, J.; Bard, A. J. *Anal. Chem.* **1989**, *61*, 1221.
(13) Saito, Y. *Rev. Polarogr. Jpn.* **1968**, *15*, 177.
(14) Bard, A. J.; Denault, G.; Dornblaser, B. C.; Friesner, R. A.; Tuckerman, L. S. *Anal. Chem.* **1991**, *63*, 1282.
(15) Albery, W. J.; Hitchman, M. L. *Ring-Disk Electrodes*; Oxford University Press: Oxford, UK, 1971.
(16) Unwin, P. R.; Compton, R. G. In *Comprehensive Chemical Kinetics*; Compton, R. G., Hammett, A., Eds.; Elsevier: Amsterdam, 1989; Vol. 29, pp 173–296.
(17) Wightman, R. M.; Wipf, D. O. In *Electroanalytical Chemistry*; Bard, A. J., Ed.; Marcel Dekker: New York, 1989; Vol. 15, pp 267–353.
(18) Wightman, R. M.; Wipf, D. O. *Acc. Chem. Res.* **1990**, *23*, 64.
(19) Wightman, R. M. In *Microelectrodes: Theory and Applications*; Montenegro, M. I., Queirós, M. A., Daschbach, J. L., Eds.; NATO ASI Ser E, Vol. 197; Kluwer: Dordrecht, 1991; p 197.
(20) Savéant, J. M. In *Microelectrodes: Theory and Applications*; Montenegro, M. I., Queirós, M. A., Daschbach, J. L., Eds.; NATO ASI Ser E, Vol. 197; Kluwer: Dordrecht, 1991; p 307.
(21) Kwak, J.; Bard, A. J. *Anal. Chem.* **1989**, *61*, 1794.
(22) Baizer, M. M. *Tetrahedron Lett.* **1963**, 973.
(23) Petrovich, J. P.; Baizer, M. M.; Ort, M. R. *J. Electrochem. Soc.* **1969**, *116*, 743.
(24) Lamy, E.; Nadjo, L.; Savéant, J. M. *J. Electroanal. Chem. Interfacial Electrochem.* **1973**, *42*, 189.
(25) Yeh, L.-S. R.; Bard, A. J. *J. Electrochem. Soc.* **1977**, *124*, 355.
(26) Puglisi, J. V.; Bard, A. J. *J. Electrochem. Soc.* **1973**, *120*, 748.
(27) Puglisi, J. V.; Bard, A. J. *J. Electrochem. Soc.* **1972**, *119*, 829.
(28) Goldberg, I. B.; Boyd, D.; Hirasama, R.; Bard, A. J. *J. Phys. Chem.* **1974**, *78*, 295.
(29) Vartines, I.; Smith, W. H.; Bard, A. J. *J. Electrochem. Soc.* **1975**, *122*, 894.
(30) Dunsch, L. In *Contemporary Electroanalytical Chemistry*; Ivaska, A., Lewenstam, A., Sara, R., Eds.; Plenum Press: New York, 1990; pp 443–452.
(31) Hubbard, A. T.; Anson, F. C. In *Electroanalytical Chemistry*; Bard, A. J., Ed.; Marcel Dekker: New York, 1970; p 129.